Asymmetric Orbital-Lattice Interactions in Ultrathin Correlated Oxide Films

J. Chakhalian,[1,*] J. M. Rondinelli,[2,3] Jian Liu,[1,4] B. A. Gray,[1] M. Kareev,[1] E. J. Moon,[1] N. Prasai,[5] J. L. Cohn,[5] M. Varela,[6]
I. C. Tung,[7] M. J. Bedzyk,[7] S. G. Altendorf,[8] F. Strigari,[8] B. Dabrowski,[9] L. H. Tjeng,[10] P. J. Ryan,[3] and J. W. Freeland[3]

[1]*Department of Physics, University of Arkansas, Fayetteville, Arkansas 70701, USA*
[2]*Department of Materials Science and Engineering, Drexel University, Philadelphia, Pennsylvania 19104, USA*
[3]*Advanced Photon Source, Argonne National Laboratory, Argonne, Illinois 60439, USA*
[4]*Advanced Light Source, Lawrence Berkeley National Laboratory, Berkeley, California 94720, USA*
[5]*Department of Physics, University of Miami, Coral Gables, Florida 33124, USA*
[6]*Oak Ridge National Laboratory, Oak Ridge, Tennessee 37831, USA*
[7]*Materials Science and Engineering, Northwestern University, Evanston, Illinois 60208, USA*
[8]*II. Physikalisches Institut, Universität zu Köln, Zülpicher Strasse 77, 50937 Köln, Germany*
[9]*Department of Physics, Northern Illinois University, Dekalb, Illinois 60115, USA*
[10]*Max Planck Institute for Chemical Physics of Solids, Nöthnitzerstrasse 40, 01187 Dresden, Germany*
(Received 8 April 2011; published 9 September 2011)

Using resonant x-ray spectroscopies combined with density functional calculations, we find an asymmetric biaxial strain-induced d-orbital response in ultrathin films of the correlated metal LaNiO$_3$ which are not accessible in the bulk. The sign of the misfit strain governs the stability of an octahedral "breathing" distortion, which, in turn, produces an emergent charge-ordered ground state with an altered ligand-hole density and bond covalency. Control of this new mechanism opens a pathway to rational orbital engineering, providing a platform for artificially designed Mott materials.

Heteroepitaxial synthesis is a powerful avenue to modify orbital-lattice interactions in correlated materials with strong electron-electron interactions derived from transition metals with open d-shell configurations [1–3]. Epitaxial strain allows access to latent electronic functionalities and phases that do not exist in bulk equilibrium phase diagrams [4–8]. However, efforts to rationally control properties that are exceedingly sensitive to small perturbations [9] through the orbital-lattice interaction are impeded by the poor understanding of how heteroepitaxy imposes constraints on the orbital response [10–12]. Despite the recent progress in strain-induced orbital engineering, a crucial fundamental question remains: When a single electron occupies a doubly degenerate d orbital in a cubic crystal field as in perovskites with Cu^{2+}, Mn^{3+}, or low-spin Ni^{3+} cations, how do the substrate-imposed epitaxial constraints dictate the correlated orbital responses of ultrathin films?

The exceptional strain control of the frontier atomic orbitals relies on the susceptibility of the orbital occupations and their energy level splittings to biaxial strain-induced lattice deformations, i.e., orbital-lattice interactions. The conventional orbital engineering approach in perovskite-structured oxides is often rationalized as follows: Coherent heteroepitaxy imposes a tetragonal distortion on the film's primitive unit cell, which then modifies the chemical bond lengths of the functional octahedral building blocks. The bond distortions in turn alter the crystal field symmetry and remove the cubic twofold e_g electron degeneracy. Since each e_g orbital state is of the same symmetry, it is generally anticipated that both tensile

and compressive strains should symmetrically alter the $d_{x^2-y^2}$ and $d_{3z^2-r^2}$ orbital states. They are either lowered or raised relative to the strain-free band center of mass, which for finite filling leads to an orbital polarization. This symmetric strain-induced orbital polarization (SIOP) concept is routinely used to rationalize the orbital responses of many complex oxide systems [12,13] and even theoretically suggested to be a possible route to replicate high-T_c cuprate physics in nickelates [14]. However, the strategies for tuning orbital ground states in *ultrathin* films devised from the supposedly symmetric strain response of the orbital occupations alone are violated more often than they apply: Doped manganite thin films exhibit $d_{3z^2-r^2}$ orbital polarization regardless of the biaxial strain sign [15,16]. Ultrathin cuprate bilayers also show variable critical temperatures [17] correlated with the sign of the interface lattice misfit [18], and cobaltite films are either ferro- or diamagnetic depending on the strain state [19].

In this Letter, we provide insight into why many ultrathin correlated oxides violate the SIOP model by investigating the orbital-lattice interactions in 10 unit cell thick films of the correlated and orbitally degenerate ($t_{2g}^6 e_g^1$) metal LaNiO$_3$ (LNO). This representative spin-$\frac{1}{2}$ system has no magnetic or structural transitions below 500 K, which otherwise might obscure the investigation [20–22]. We identify the microscopic mechanism responsible for the asymmetric strain-induced orbital response and show that it originates from latent instabilities of the bulk material, which are strongly enhanced due to the epitaxial constraints imposed by the heterointerface. We further

demonstrate deterministic control of the ligand-hole density and covalency through the asymmetric orbital-lattice response, enabling access to an emergent charge-ordered phase not attainable in the bulk.

For this purpose, we synthesized high quality epitaxial LaNiO$_3$ films under different strain states by pulsed laser deposition on (001)-oriented single crystal LaAlO$_3$ (LAO, lattice mismatch of -1.08%), SrLaGaO$_4$ (SLGO, $+0.31\%$), SrTiO$_3$ (STO, $+1.83\%$), and GdScO$_3$ (GSO, $+3.6\%$) substrates. Synchrotron-based x-ray diffraction confirms the LNO films are fully and homogeneously strained [23]. Consistent with previous studies on rhombohedral perovskites [24,25], we find our films have lower (monoclinic) symmetry than that of the bulk.

Figure 1(a) reveals a large anisotropy in the galvanoelectric response with the sign of the strain. On the tensile side, the inverse Hall coefficient R_H^{-1} is small and independent of lattice mismatch indicating nearly zero strain modulation in the carrier density, while for compressive strain an order of magnitude increase in R_H^{-1} occurs. In addition, Fig. 1(b) shows the thermoelectric power (TEP) over a broad temperature range from 300 down to 1.5 K for LNO films under different strain states. The thermopower in films on the tensile side lacks any noticeable anomalies and follows the Mott relation [26], though the magnitude is shifted relative to the bulk toward positive values. For compressive strain, the magnitude is comparable to the bulk at $T > 80$ K, but a different temperature dependence emerges at low T: Namely, a large negative peak, reminiscent of phonon drag, occurs at 25 K. The asymmetric strain-induced TEP response indicates distinct differences in the electronic structure under tensile and compressive strain. In contrast, hydrostatic pressure produces only modest enhancements in the TEP magnitude [Fig. 1(b)], indicating compressive biaxial strain is inequivalent to hydrostatic pressure.

To explore the microscopic origins of the asymmetric strain-induced electronic states, we probe the local
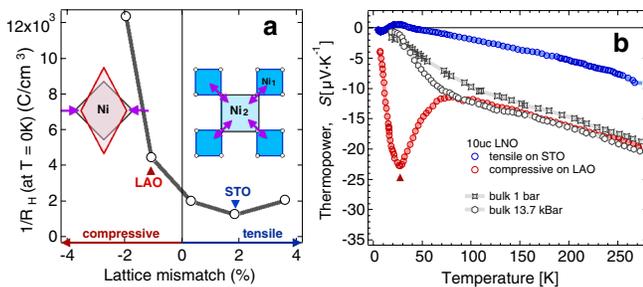
occupied 3d orbital configurations and the oxygen-derived states by using both x-ray absorption spectroscopy (XAS) and x-ray linear dichroism (XLD) measurements at the Ni L and O K edges. Figures 2(a)–2(c) show the normalized room temperature XAS spectra at the Ni $L_{3,2}$ edge for polarization oriented parallel to a-b vs c axes under different epitaxial strain states. Here, we focus on two representative films under (on) compressive (LAO) and tensile (STO) strain states (substrates). Each polarization-averaged spectra is representative of octahedrally coordinated Ni^{3+} in good agreement with the valence of bulk LNO. There are distinct differences, however, in the polarization dependence between films under compressive and tensile strain: The absorption for photon polarization perpendicular to the NiO$_2$ sheets is shifted ~ 0.1 eV lower in energy than the in-plane polarization (a-b) for LNO under compressive strain on LAO [Fig. 2(a)]. The dichroism indicates a small conduction band splitting Δe_g between the Ni-derived $d_{x^2-y^2}$ and $d_{3z^2-r^2}$ orbitals (Fig. 2, right) due to the distortion of the spherical charge distribution around the Ni sites by nonuniform Ni-O bond lengths. The sign of the XLD implies that the in-plane Ni-O bonds are moderately compressed relative to the out-of-plane apical Ni-O bonds along the c axis in agreement with both the model of *symmetric* SIOP and the measured axial ratio for the films on LAO.

For STO with the same substrate-film orientation but strain of the opposite sign, the SIOP model predicts an inversion of the orbital polarization and the population of the $d_{x^2-y^2}$ orbital; however, consistent with our measured R_H^{-1} and TEP, the polarization dependence of the films
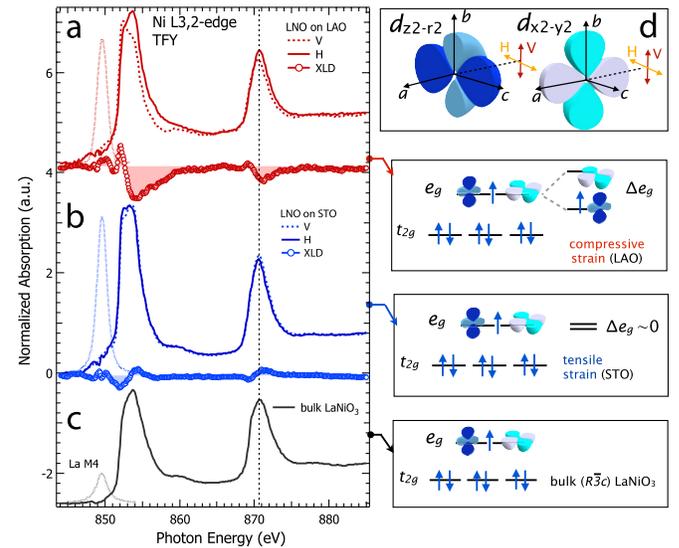

FIG. 1 (color online). Asymmetric strain-induced responses: (a) inverse Hall coefficient R_H^{-1} and (b) temperature-dependent TEP. The carrier-density modulation in perovskite oxides is intimately linked with the local structure of the NiO$_6$ octahedra (inset). The TEP in (b) reveals that epitaxial strain and hydrostatic (bulk LNO under 1 bar and 13 kbar) pressure are inequivalent. Bulk data are from Ref. [32].

FIG. 2 (color online). Normalized absorption spectra at the Ni L edge (fluorescence mode) with varying photon polarization (see the legend) for films under (a) compressive and (b) tensile strain, on LAO and STO substrates, respectively, and (c) bulk (ceramic) LNO. (right) Schematic orbital level diagram for bulk LNO and the inferred SIOP effect on the e_g doublet.

under tensile strain is remarkably different. Figure 2(b) shows the orbital dichroism is absent, suggesting that uniform Ni-O bond lengths and a highly symmetric cubic crystal field ($\Delta e_g \sim 0$) remain seemingly intact despite the large ($\sim 2\%$) tensile strain. These findings are surprising as the in-plane lattice parameters are expanded by 2% and, due to coherent film registry with substrate, the symmetric SIOP should have produced a large orbital polarization.

To elucidate how the strain-stabilized film structure produces an asymmetric orbital polarization, we perform density functional calculations within the local-spin density approximation plus Hubbard U method following the details in Ref. [25]. We carry out structural optimizations for homoepitaxially strained nickelate films using our experimentally determined lattice parameters. We find that samples under compressive strain have an atomic structure characterized by Ni-O-Ni bond angles, which are larger within the epitaxial xy plane than those along the growth (z) direction. The structure also consists of a single Ni^{3+} site with different in-plane and out-of-plane Ni-O bond lengths that lift the formerly bulk D_{3d} Ni-site symmetry.

Films under tensile strain exhibit rotated octahedra but with an additional intriguing *breathing* distortion imposed on the NiO_6 octahedra [Fig. 1(inset)]. The breathing octahedral distortion induces a Ni-O bond length disproportionation and splits the formerly bulk equivalent Ni sites into Ni(1) and Ni(2). They are located at the center of nearly ideal NiO_6 octahedra with average in-plane and out-of-plane bonds lengths of 2.00 and 1.93 Å, respectively. Interestingly, an analogous tendency to bond disproportionation leading to charge disproportionation of the type $Ni^{(3\pm\delta)+}$ is present in the low-temperature monoclinic phases of small rare-earth nickelates [27,28] but not for bulk LNO. Note that the NiO_6 octahedral breathing distortion is unstable for compressive strain—a single Ni^{3+} site is preferred.

We next compare the electronic ground state of LNO on LAO and STO with the bulk electronic structure. For films under compressive strain [Fig. 3(a)], we find a strain-induced crystal field splitting of the Ni $3d$ orbitals with an electronic structure that remains metallic, as in the bulk [Fig. 3(b)], albeit with a strongly increased bandwidth of ~ 0.20 eV. We find that the low-spin Ni^{3+} electronic configuration is accurately described as itinerant and strongly mixed with an oxygen ligand hole, $d^8\underline{L}$. In sharp contrast, films under tensile strain on STO show a semiconducting gap of 0.10 eV with the bottom of the valence band edge shifted by ~ 0.5 eV over the compressively strained film [Figs. 3(c) and 3(d)]. We observe a modulation in the Ni-O bond covalency through the $dp\sigma$ band splitting, which produces an energy gap between the antibonding e_g orbitals, that is stabilized by the emergent strain-induced octahedral breathing distortion not found in the bulk.

Figures 3(c) and 3(d) show that the valence band of LNO under tensile strain is primarily composed of the e_g states
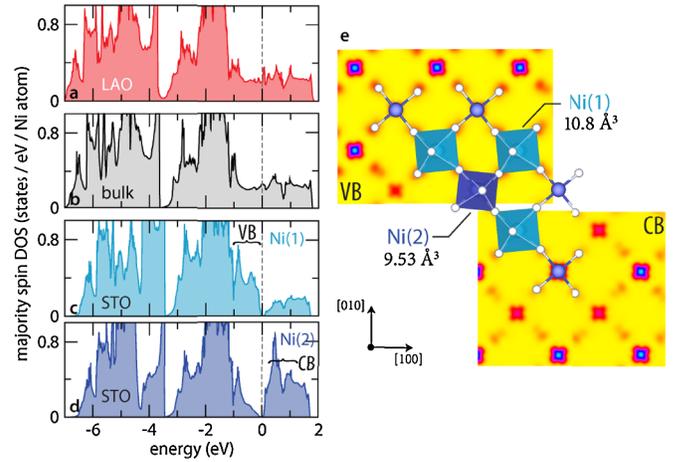

FIG. 3 (color online).   The majority spin Ni $3d$ density of states (DOS) for LNO on (a) a LAO substrate; for (b), a strain-free bulk crystal; and on (c) and (d) the STO substrate. (e) The electron density for LNO on STO in the NiO_2 epitaxial plane [values integrated between -0.70 and 0 eV (denoted as valence band, VB) and 0 and 1.7 eV (denoted as conduction band, CB)] reveals the 3D checkerboard spatial distribution of the Ni e_g states derived from the small and large octahedral units. [Darker (blue) areas indicate a higher value of the charge density.]

from the more ionic Ni(1) cation with nearly one electron in each $d_{x^2-y^2}$ and $d_{3z^2-r^2}$ atomic orbital ($S = 1$). The suppressed intensity at the valence band edge indicates that this orbital occupation is due to charge transfer from the covalent Ni(2) site to the larger and more ionic Ni(1) site. We calculate the charge transfer δ between Ni sites to be $\sim 0.20e$ and homogeneously ordered throughout the film [Fig. 3(e)]. Because δ is small and the low-spin Ni^{3+} valence is rare, it is equally likely that a bond-centered double ligand-hole $\underline{L}$ state, similar to the Zhang-Rice states in hole doped cuprates [29], could be stabilized over the site-centered configuration. Nonetheless, our XLD data and first-principles calculations show that, for LNO films under tension, the preferred electronic configuration is one *without* a net d-orbital polarization. The semi-ionic state results from a charge density modulation that occurs in the presence of orbital level splittings induced by tensile strain; in contrast, compressive strain favors a uniform orbital polarization of the Ni sites.

To evaluate the degree of strain-modulated covalency, we use resonant XAS measurements at the oxygen K edge to isolate the change in the ligand-hole density of the $d^8\underline{L}$ component of the Ni^{3+} ground state. The oxygen spectrum around 528.5 eV corresponds to transitions from the core-level O $1s$ state into the unoccupied and strongly hybridized O $2p$–Ni $3d$ states [Fig. 4(a)]; the observed prepeak intensity provides a direct measure of the degree of Ni-O bonding. Unlike the Ni L edge, which is well aligned to the bulk LNO value, the oxygen prepeak reveals a remarkably systematic and nearly linear dependence of the peak position with strain [Fig. 4(b)]: It shifts at a rate of almost 100 meV
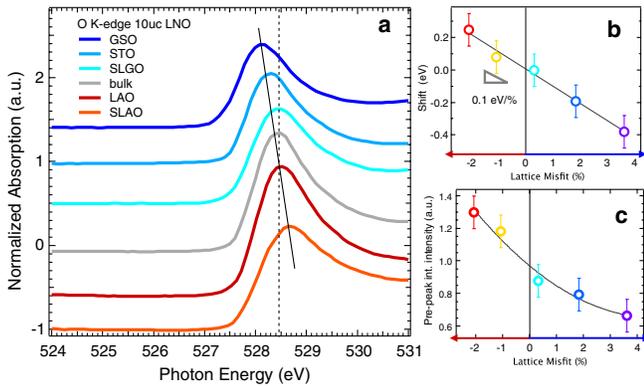
FIG. 4 (color online). Biaxial strain-induced covalency changes: (a) Low energy O K-edge prepeak absorption around 528.5 eV for compressive (red) and a range of tensile (shades of blue) strain states (a.u., arbitrary units). We omit peaks above 530 eV (transitions into La $5d4f$ and Ni $4s4p$ states) for clarity. (b) Energy shift and (c) the normalized FWHM relative to the bulk LNO energy position with misfit strain.

per percent lattice misfit, indicating direct strain control of the ligand-hole density. Figure 4(c) shows a corresponding systematic change in the full width at half maximum (FWHM), suggesting a strong narrowing of the electron bandwidth due to the deviation of the Ni-O-Ni bond angle away from the ideal 180° with increasing tensile strain.

In charge transfer oxides like nickelates and cuprates, the position of the O K-edge prepeak directly couples to the charge transfer energy, which is also highly susceptible to the symmetry of the cation coordination [30]. The strain-stabilized atomic distortions should therefore modify the Madelung energy. The constant nickel valence across all strain states explored allows us to probe the limits of the cohesive energy tunability with x-ray photoemission spectroscopy. Indeed, we find a controllable modulation of the O $1s$ core-level energy by ~ 0.29 eV between LNO on LAO and STO (0.16 eV per percent strain) due to the asymmetric orbital-lattice interactions in agreement with our XAS results and calculations [23]. These experimental findings demonstrate that strain control of the ligand-hole density is due to a major Madelung energy response. We conjecture that, by reversibly accessing these asymmetric orbital-lattice interactions, control of the charge transfer energy and d-orbital polarization should enable access to latent metal-insulator phase transitions in other classes of correlated electron systems [31].

In summary, using a combination of resonant x-ray spectroscopies and first-principles calculations, we report the discovery of a fundamental asymmetry in the hetero-epitaxial strain-induced orbital occupation response of ultrathin perovskite films with orbitally degenerate transition metal ions. We suggest that knowledge of this asymmetric orbital-lattice interaction is fundamental to the rational design of quantum materials with exotic correlated phases and enhanced critical temperatures.

*jchakhal@uark.edu
[1] H. Takagi and H. Hwang, Science **327**, 1601 (2010).
[2] J. Mannhart and D. Schlom, Science **327**, 1607 (2010).
[3] S. Hormoz and S. Ramanathan, Solid State Electron. **54**, 654 (2010).
[4] J. H. Lee et al., Nature (London) **466**, 954 (2010).
[5] J. Cao et al., Nature Nanotech. **4**, 732 (2009).
[6] R. J. Zeches et al., Science **326**, 977 (2009).
[7] Y. Wakabayashi et al., Phys. Rev. Lett. **96**, 017202 (2006).
[8] S. Okamoto and A. J. Millis, Nature (London) **428**, 630 (2004).
[9] E. Dagotto, Science **309**, 257 (2005).
[10] E. Benckiser et al., Nature Mater. **10**, 189 (2011).
[11] A. V. Boris et al., Science **332**, 937 (2011).
[12] Y. Tokura and N. Nagaosa, Science **288**, 462 (2000).
[13] K. Ahn, T. Lookman, and A. Bishop, Nature (London) **428**, 401 (2004).
[14] J. Chaloupka and G. Khaliullin, Phys. Rev. Lett. **100**, 016404 (2008);P. Hansmann et al., Phys. Rev. Lett. **103**, 016401 (2009); P. Hansmann et al., Phys. Rev. B **82**, 235123 (2010).
[15] D. Khomskii and J. van den Brink, Phys. Rev. Lett. **85**, 3329 (2000).
[16] A. Tebano et al., Phys. Rev. Lett. **100**, 137401 (2008).
[17] A. Gozar et al., Nature (London) **455**, 782 (2008).
[18] H. Zhou et al., Proc. Natl. Acad. Sci. U.S.A. **107**, 8103 (2010).
[19] D. Fuchs et al., Phys. Rev. B **77**, 014434 (2008).
[20] J. L. Garcia-Munoz, J. Rodriguez-Carvajal, P. Lacorre, and J. B. Torrance, Phys. Rev. B **46**, 4414 (1992).
[21] J. B. Torrance et al., Phys. Rev. B **45**, 8209 (1992).
[22] J.-S. Zhou et al., Phys. Rev. Lett. **84**, 526 (2000).
[23] See Supplemental Material at http://link.aps.org/supplemental/10.1103/PhysRevLett.107.116805 for film growth procedures, structural and spectroscopic characterizations, and complete computational details.
[24] A. Vailionis et al., Phys. Rev. B **83**, 064101 (2011).
[25] S. J. May et al., Phys. Rev. B **82**, 014110 (2010).
[26] N. F. Mott and H. Jones, The Theory of the Properties of Metals and Alloys (Clarendon, Oxford, 1936).
[27] G. Catalan, Phase Transit. **81**, 729 (2008).
[28] J. L. Garcia-Munoz, M. A. G. Aranda, J. A. Alonso, and M. J. Martinez-Lope, Phys. Rev. B **79**, 134432 (2009).
[29] F. C. Zhang and T. M. Rice, Phys. Rev. B **37**, 3759 (1988).
[30] M. Alexander et al., Phys. Rev. B **43**, 333 (1991).
[31] J. Liu et al., Appl. Phys. Lett. **96**, 233110 (2010).
[32] J.-S. Zhou et al., Phys. Rev. B **61**, 4401 (2000).